JACS
JOURNAL OF THE AMERICAN CHEMICAL SOCIETY

COMMUNICATION

pubs.acs.org/JACS

Reduced Graphene Oxide as a Solid-State Electron Mediator in Z-Scheme Photocatalytic Water Splitting under Visible Light

Akihide Iwase,[†,§] Yun Hau Ng,[†,§] Yoshimi Ishiguro,[‡] Akihiko Kudo,[‡] and Rose Amal*[,†]

[†]ARC Centre of Excellence for Functional Nanomaterials, School of Chemical Engineering, The University of New South Wales, Sydney, NSW 2052, Australia

[‡]Department of Applied Chemistry, Faculty of Science, Tokyo University of Science, 1-3 Kagurazaka, Shinjuku-ku, Tokyo 162-8601, Japan

Supporting Information

ABSTRACT: The effectiveness of reduced graphene oxide as a solid electron mediator for water splitting in the Z-scheme photocatalysis system is demonstrated. We show that a tailor-made, photoreduced graphene oxide can shuttle photogenerated electrons from an O_2-evolving photocatalyst ($BiVO_4$) to a H_2-evolving photocatalyst (Ru/$SrTiO_3$:Rh), tripling the consumption of electron−hole pairs in the water splitting reaction under visible-light irradiation.

Production of clean hydrogen fuel from water using sunlight is one of the promising solutions to address the increasing demand for energy and associated environmental concerns. Two methods currently dominate research on splitting of water into H_2 and O_2 by photocatalysis: photoelectrochemical[1−6] and powdered photocatalytic[5,7−10] water splitting. Generally, a photoelectrochemical system involves a rather complicated cell setup that requires the application of an applied bias and an expensive platinum counter electrode; scale-up attempts are always limited by the exposed area of the photoelectrodes. A powdered-type photocatalytic method that requires only a water pool containing photocatalyst powders offers an interesting opportunity to generate H_2 in a more energy-efficient manner. For the powdered photocatalytic water splitting reaction, two approaches have been reported. The first approach is the development of a single photocatalyst with sufficient potential to achieve overall water splitting.[5,7−12] Although a number of photocatalysts have been found to be active in splitting water, most of them are responsive only to UV illumination.[5,7−10] Oxynitride solid-solution photocatalysts, such as $(Ga_{1-x}Zn_x)(N_{1-x}O_x)$ and $(Zn_{1+x}Ge)(O_xN_2)$, are currently the most established single photocatalysts that work under visible-light irradiation.[11,12] The second approach is the construction of a two-step photoexcitation system, often called a Z-scheme photocatalysis system, that mimics natural photosynthesis.[13−22] A Z-scheme system employs two photocatalysts, one producing H_2 (the H_2 photocatalyst) and the other O_2 (the O_2 photocatalyst), usually with the aid of an electron shuttle.[9]

The Z-scheme photocatalytic system has greater potential to work under sunlight, as an increasing number of visible-light-active H_2 and O_2 photocatalysts have been developed separately with the proper sacrificial electron donors or acceptors. Neither a H_2 photocatalyst nor an O_2 photocatalyst can function independently to split water into H_2 and O_2. When the two are combined, however, electrons generated in the O_2 photocatalyst can be transferred to holes in the excited H_2 photocatalyst, allowing the oxidation and reduction of water to take place on the O_2 and H_2 photocatalysts, respectively. Recent development of the Z-scheme system has suggested that electron transfer between the two photocatalysts is the rate-determining process.[21] Therefore, the presence of an electron transporter is critical to boost effective electron relay. The Fe^{3+}/Fe^{2+}[13,16,18] and IO_3^-/I^-[15,17,19,20,22] redox couples are the most commonly employed electron mediators for shuttling electrons from the O_2 to the H_2 photocatalyst. Although these ionic redox couples perform efficiently in relaying electrons, a solid electron mediator is more favorable in terms of recovery of the photocatalyst and reclamation of clean water. The challenge in developing a solid-state electron mediator lies in achieving a dynamic equilibrium between the electron-accepting and -donating abilities of the mediator, allowing it to remain relatively unchanged during reaction. The photocatalyst−mediator−photocatalyst contact interface is another crucial factor in ensuring a continuous flow of electrons between the source and target photocatalysts.

We recently demonstrated that photoreduced graphene oxide (PRGO) improves the photoelectrochemical performance of $BiVO_4$ and TiO_2 photoanodes by providing low-resistance electron pathways to the external circuit under an applied bias.[23,24] Also, Kamat and co-workers demonstrated that PRGO carries electrons photogenerated in a TiO_2 photocatalyst to reduce Ag^+ ions.[25] Because of its large two-dimensional matlike structure with a size of several micrometers, the possibility of using PRGO as the conductive medium to interface the H_2 and O_2 photocatalysts prompted us to investigate its function as an interparticulate electron mediator. We report herein that fine-tuning of the PRGO/semiconductor composite allows PRGO to be used as a solid electron mediator for Z-scheme photocatalytic water splitting using $BiVO_4$ and Ru/$SrTiO_3$:Rh as the O_2 and H_2 photocatalysts, respectively.

Mixtures of PRGO with $BiVO_4$ (PRGO/$BiVO_4$) and Ru/$SrTiO_3$:Rh (PRGO/Ru/$SrTiO_3$:Rh) were prepared by photocatalytic reduction of GO on $BiVO_4$ and Ru/$SrTiO_3$:Rh, respectively, under visible-light illumination in the presence of methanol as a hole scavenger. To assess the effectiveness of this photocatalytic reduction of GO, a chemical reduction method

Received: April 10, 2011
Published: June 28, 2011

using hydrazine was also performed. Figure 1 shows C 1s X-ray photoelectron spectroscopy (XPS) data for the original GO, hydrazine-reduced GO (N_2H_4-RGO), PRGO/$BiVO_4$, and PRGO/Ru/$SrTiO_3$:Rh. All of the samples exhibited three peaks due to carbon species with different surroundings: C−C, C−O, and C=O.[24] The degree of GO reduction was monitored by the oxygen-bound carbon content, which was calculated using eq 1:

$$\% \text{ O-bound C} = \frac{A_{C-O} + A_{C=O}}{A_{C-C} + A_{C-O} + A_{C=O}} \times 100\% \tag{1}$$

where A_{C-C}, A_{C-O}, and $A_{C=O}$ are the peak areas for graphitic (C−C) and O-bound (C−O and C=O) carbon, respectively. GO as the precursor contained 43% O-bound carbon, revealing fairly effective oxidation of the commercial graphite. Reaction of GO with hydrazine and the O_2 and H_2 photocatalysts resulted in different degrees of reduction, as indicated by their O-bound C contents (Figure 1 inset). The O-bound C content of N_2H_2-RGO decreased drastically relative to GO (9 vs 43%) as expected, while Ru/$SrTiO_3$:Rh and $BiVO_4$ also clearly demonstrated their capabilities in reducing or partially reducing GO to PRGO (O-bound C content = 10% for Ru/$SrTiO_3$:Rh and 28% for $BiVO_4$). The higher degree of GO reduction using Ru/$SrTiO_3$:Rh in comparison with $BiVO_4$ is due to the higher conduction-band energy of Ru/$SrTiO_3$:Rh and the presence of the Ru cocatalyst as highly reductive sites.

Table 1 shows the activity of the Z-scheme systems constructed using various combinations of Ru/$SrTiO_3$:Rh, $BiVO_4$, and reduced GO under visible-light illumination. No water splitting was observed when the activity of Ru/$SrTiO_3$:Rh or $BiVO_4$ alone was measured in the nonsacrificial condition, either with or without PRGO (entries 1−4). When the two were combined (entry 5), H_2 and O_2 evolved at a steady rate through interparticulate charge transfer. Interacting PRGO/$BiVO_4$ with Ru/$SrTiO_3$:Rh led to a 3-fold enhancement in the gas evolution (entry 8). This improvement is attributable to the presence of PRGO to receive excited electrons from $BiVO_4$ (the O_2 photocatalyst) and release them to Ru/$SrTiO_3$:Rh (the H_2 photocatalyst). This mechanism of electron flow increased the charge separation efficiency in each photocatalyst, leaving holes in $BiVO_4$ and electrons in Ru/$SrTiO_3$:Rh to split the water. Although the exact mechanism has not yet been clarified, the electrons mainly flow from $BiVO_4$ to Ru/$SrTiO_3$:Rh.

We also measured the apparent quantum yield efficiencies obtained with monochromatic light at 420 nm.[26] The efficiencies of the Z-scheme systems consisting of Ru/$SrTiO_3$:Rh and $BiVO_4$ in the presence and absence of PRGO prepared by $BiVO_4$ were 1.03 and 0.97% at 420 nm, respectively. Although the gas evolution was greatly enhanced in the presence of PRGO under full-range visible-light illumination from the Xe lamp (Table 1, entries 5 and 8), the apparent quantum yield efficiencies showed only a modest difference. When the apparent quantum yield efficiency is measured using low-intensity monochromatic light, which generates only a limited number of electron−hole pairs, interparticle charge transfer between Ru/$SrTiO_3$:Rh and $BiVO_4$ is not the rate-controlling step. Therefore, only a small enhancement was observed in the apparent quantum yield efficiency when PRGO was incorporated. In contrast, as a more practical full-range visible-light irradiation with higher intensity produces a large number of electron−hole pairs, interparticulate electron transfer from $BiVO_4$ to Ru/$SrTiO_3$:Rh determines the overall rate of water splitting activity. The presence of PRGO overcomes the limitation of interparticulate transfer of populated electrons and holes, thus resulting in a great improvement in the photocatalytic activity. This argument is well-supported by the fact that the enhancement by PRGO disappeared when we reduced the light intensity to 20% using a neutral density filter.

Figure 2 shows the time courses of H_2 and O_2 evolution from a mixture of PRGO/$BiVO_4$ and Ru/$SrTiO_3$:Rh in acidified water (pH 3.5) under visible-light illumination. The reactions were conducted for 24 h with two intermediate evacuations after every 8 h of irradiation. The activity during the second cycle was slightly decreased, as is normally observed for most systems, and the activity at third cycle was almost the same as that of the second cycle, implying a stable system after the second cycle. The minimum turnover number (TON), calculated as the number of moles of reactive electrons per mole of PRGO (assumed to contain pristine graphitic carbon[27]) was found to be 3.2 over 24 h. This value is comparable that for the system employing Fe^{3+}/Fe^{2+} (TON of 2 over 22 h),[18] evidently proving the suitability of

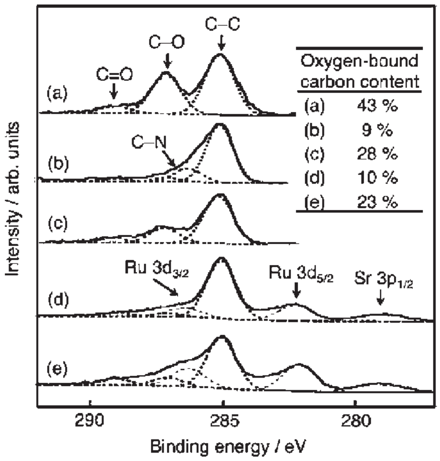

Figure 1. C 1s XPS spectra for (a) graphene oxide (GO), (b) hydrazine-reduced GO, (c) GO photoreduced by $BiVO_4$, (d) GO photoreduced by Ru/$SrTiO_3$:Rh, and (e) (Ru/$SrTiO_3$:Rh)−(PRGO/$BiVO_4$) after reaction. Inset: O-bound C contents calculated using eq 1.

Table 1. Overall Water Splitting under Visible-Light Irradiation by the (Ru/$SrTiO_3$:Rh)−($BiVO_4$) System in the Presence and Absence of Photoreduced Graphene Oxide[a]

entry	H_2 photocat.	reduced GO[b]	O_2 photocat.	pH	activity (μmol) H_2	activity (μmol) O_2
1	Ru/$SrTiO_3$:Rh	–	–	3.5	0.9	0
2	Ru/$SrTiO_3$:Rh	PRGO(Ru/$SrTiO_3$:Rh)	–	3.5	0.9	0
3	–	–	$BiVO_4$	3.5	0	0
4	–	PRGO($BiVO_4$)	$BiVO_4$	3.5	0	0
5	Ru/$SrTiO_3$:Rh	–	$BiVO_4$	3.5	3.7	1.9
6	Ru/$SrTiO_3$:Rh	–	$BiVO_4$	7.0	0.8	0.5
7	Ru/$SrTiO_3$:Rh	PRGO(Ru/$SrTiO_3$:Rh)	$BiVO_4$	3.5	1.4	0.6
8	Ru/$SrTiO_3$:Rh	PRGO($BiVO_4$)	$BiVO_4$	3.5	11	5.5
9	Ru/$SrTiO_3$:Rh	PRGO($BiVO_4$)	$BiVO_4$	7.0	1.1	0.6
10	Ru/$SrTiO_3$:Rh	N_2H_4-RGO	$BiVO_4$	3.5	4.8	2.3

[a] Conditions: photocatalysts (0.03 g each) in water or H_2SO_4(aq) (120 mL); light source, 300 W Xe lamp (λ > 420 nm); top-irradiation cell with a Pyrex window. [b] PRGO(Ru/$SrTiO_3$:Rh) and PRGO($BiVO_4$), denote graphene oxide (GO) photoreduced by Ru/$SrTiO_3$:Rh and $BiVO_4$, respectively; N_2H_4-RGO denotes GO reduced by hydrazine.

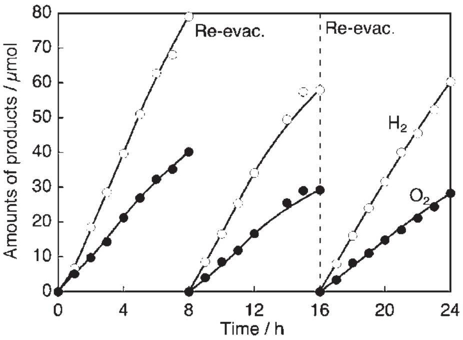

Figure 2. Overall water splitting under visible-light irradiation by the ($Ru/SrTiO_3$:Rh)−($PRGO/BiVO_4$) system. Conditions: catalysts (0.03 g each) in H_2SO_4(aq) (pH 3.5, 120 mL); light source, 300 W Xe lamp with a 420 nm cutoff filter; top-irradiation cell with a Pyrex glass window.

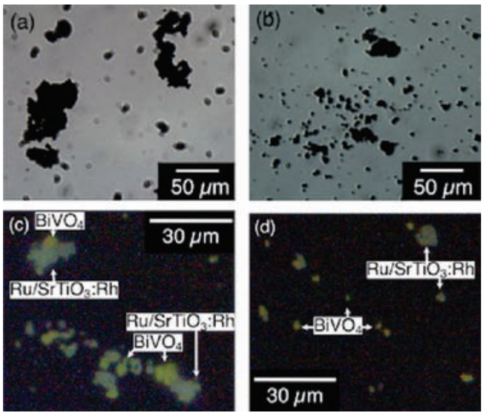

Figure 3. Optical microscopy images of $Ru/SrTiO_3$:Rh and $PRGO/BiVO_4$ suspended in water at (a, c) pH 3.5 adjusted by H_2SO_4 and (b, d) pH 7.0.

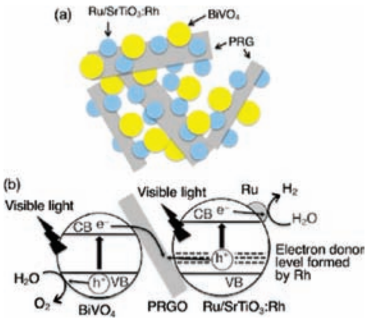

Figure 4. (a) Schematic image of a suspension of $Ru/SrTiO_3$ and $PRGO/BiVO_4$ in water at pH 3.5. (b) Mechanism of water splitting in a Z-scheme photocatalysis system consisting of $Ru/SrTiO_3$:Rh and $PRGO/BiVO_4$ under visible-light irradiation.

PRGO as a solid electron mediator. This TON value larger than unity and the H_2 and O_2 evolution in a stoichiometric ratio indicate that this Z-scheme system split water photocatalytically and suggest that PRGO is stable as an electron mediator over a period of 24 h. The stability of PRGO is supported by the XPS results shown in Figure 1e, which indicated that the PRGO did not undergo oxidation/decomposition by the photogenerated holes from the two photocatalysts.

Interestingly, while PRGO prepared by $BiVO_4$ tripled the water splitting, the activity was retarded to a level below the non-PRGO system when PRGO prepared by $Ru/SrTiO_3$:Rh was used (entry 7). On the basis of the XPS results, unlike the partially reduced PRGO prepared by $BiVO_4$ (28% O-bound carbon), $PRGO/Ru/SrTiO_3$:Rh restored most of its graphitic carbon (only 10% O-bound carbon remained). This efficient photoreduction of GO, although in most cases desirable, imparted strong hydrophobicity to the $PRGO/Ru/SrTiO_3$:Rh particles, making them immiscible in water. This was visualized in the experiment: $PRGO/Ru/SrTiO_3$:Rh particles were seen floating on the water surface, while $BiVO_4$ particles were suspended in the water during reaction [Figure S2 in the Supporting Information (SI)]. This lack of interparticulate contact between H_2 and O_2 photocatalysts led to limited gas generation. To provide further evidence for the hydrophobicity effect of RGO in this Z-scheme photocatalytic system, hydrophobic N_2H_4-RGO was employed as the mediator (entry 10). Activity similar to that of the non-RGO system, together with the observation of poor dispersion of the N_2H_2-RGO in water, revealed the importance of RGO miscibility in water in addition to good electron-transport properties. Therefore, to achieve the best balance between the extent of GO reduction and the hydrophobicity is a crucial factor in determining its proper function as an electron mediator in a Z-scheme photocatalytic water splitting system. It was confirmed that unlike $PRGO/Ru/SrTiO_3$:Rh, $PRGO/BiVO_4$, which enhanced the activity, can disperse well in water (Figure S2d).

Since intimate physical interaction between the H_2 and O_2 photocatalysts must occur to allow the charge transfer, the surface charges of $Ru/SrTiO_3$:Rh and $PRGO/BiVO_4$ were adjusted by pH to induce aggregation within the photocatalysts. Similar to the previous findings for bare $BiVO_4$ and $Ru/SrTiO_3$,[21] Figure 3 shows that $PRGO/BiVO_4$ and $Ru/SrTiO_3$:Rh photocatalysts were aggregated at pH 3.5 but remained dispersed at pH 7. Reflectance mode images obtained from the optical microscope indicated the location of $PRGO/BiVO_4$ and $Ru/SrTiO_3$:Rh. From the ζ potential (Figure S3), this aggregation was caused by the electrostatic interaction between the surface charges of $Ru/SrTiO_3$:Rh and $PRGO/BiVO_4$ at different pH (i.e., attractive at pH 3.5 but repulsive at pH 7). As a result of this close assembly of PRGO and the O_2 and H_2 photocatalysts, the water splitting activity was tripled at pH 3.5 (entries 5 and 8). However, distantly dispersed $PRGO/BiVO_4$ and $Ru/SrTiO_3$:Rh at pH 7 showed negligible variance between the systems with and without PRGO (entries 6 and 9). Scanning electron microscopy (SEM) was also employed to observe that $PRGO/BiVO_4$ and $Ru/SrTiO_3$:Rh do exist as a composite on the PRGO. Figure S4d shows the SEM image of $Ru/SrTiO_3$:Rh and $PRGO/BiVO_4$ obtained from the pH 3.5 suspension. Both $Ru/SrTiO_3$:Rh and $BiVO_4$ particles were seen to be integrated with PRGO. Although this image may not represent the exact agglomeration of these particles in the reaction suspension, on the basis of the activity improvement and optical images of the suspension, we believe it reflects a reasonable approximation of the aggregation state.

Figure 4 shows a proposed mechanism for the activity of PRGO as a solid-state electron mediator in a Z-scheme photocatalytic water splitting system. The $PRGO/BiVO_4$ (O_2 photocatalyst) and $Ru/SrTiO_3$:Rh (H_2 photocatalyst) are attracted to each other by surface charge modulation under acidic conditions (pH 3.5), as depicted in Figure 4a. Upon excitation with visible light, electrons are photoexcited from the valence band ($BiVO_4$) or an impurity level formed by Rh ($Ru/SrTiO_3$:Rh) to the conduction band. On the basis of the UV−vis spectrum of PRGO/$BiVO_4$ (Figure S1), the absence of an absorption edge for PRGO indicates that the PRGO in the current system does not have an energy gap. Moreover, the PRGO powder showed a sheet resistance of 6.14 kΩ/□, which is comparable with the value of 6.85 kΩ/□ for graphite (see the SI); a conductor usually does not have an energy gap. These indicate that the PRGO does not contribute to the generation of electrons and holes by absorption of visible light. In other words, the RGO in this work behaves as an electron conductor. PRGO transfers the electrons from the conduction band of $BiVO_4$ to the vacancies in the impurity levels of Ru/$SrTiO_3$:Rh. Simultaneously, the electrons in Ru/$SrTiO_3$:Rh reduce water to H_2 on the Ru cocatalyst, while the holes in $BiVO_4$ oxidize water to O_2, accomplishing a complete water splitting cycle. This electron flow direction is supported by our previous study on the $BiVO_4$−PRGO photoelectrode system:[24] the PRGO provides pathways for electrons photogenerated in the $BiVO_4$ photocatalyst to reach the electrode substrate, which subsequently reduces water to H_2 on the counter electrode while the holes oxidize water to O_2 on the $BiVO_4$ surface. Unlike the photoelectrode system, where electron flow is driven by an external bias, it is electrodynamically possible to flow electrons through the PRGO in the opposite direction (from Ru/$SrTiO_3$:Rh to $BiVO_4$) in the current system. However, the driving force for this opposite electron flow is suppressed by two factors. The first involves electrons in the conduction band of Ru/$SrTiO_3$:Rh and holes in the valence band of $BiVO_4$. Each of these can migrate in two ways: reduction of water and transfer to PRGO for electrons and oxidization of water and transfer to PRGO for holes. Since the majority of the photocatalysts' surfaces are surrounded by water (reactant) and only relatively small portions are in contact with PRGO, most of the electrons in Ru/$SrTiO_3$:Rh and holes in $BiVO_4$ are consumed for water splitting. The second factor involves electrons in the conduction band of $BiVO_4$ and holes in the electron-donor level of Ru/$SrTiO_3$:Rh. To undergo recombination, electrons in $BiVO_4$ must migrate to holes in Ru/$SrTiO_3$:Rh through PRGO because electrons in $BiVO_4$ and holes in Ru/$SrTiO_3$:Rh cannot reduce and oxidize water, respectively.[28]

In conclusion, we have demonstrated that photoreduced graphene oxide prepared using $BiVO_4$ can be used as a solid-state electron mediator for a Z-scheme photocatalytic water splitting system. Unlike hydrazine-reduced GO and GO photocatalytically reduced by Ru/$SrTiO_3$:Rh, which exhibit significant hydrophobicity, GO photoreduced by $BiVO_4$ is miscible in water and provides a great improvement in the activity for water splitting by efficiently transferring photoexcited electrons from the O_2 photocatalyst to the H_2 photocatalyst. The key factor that enables efficient electron transfer in a Z-scheme system lies in achieving a balance between the degree of GO reduction (for conductivity restoration) and the level of hydrophobicity. The PRGO prepared by $BiVO_4$ demonstrated in this work possesses a high electron conductivity and a low degree of hydrophobicity. The present study has paved a new way of using the attractive graphitic carbon material graphene in the design of new and efficient systems for water splitting.

■ ASSOCIATED CONTENT

Ⓢ Supporting Information. Additional figures and experimental procedures. This material is available free of charge via the Internet at http://pubs.acs.org.

■ AUTHOR INFORMATION

Corresponding Author

r.amal@unsw.edu.au

Author Contributions

[§]These authors contributed equally.

■ ACKNOWLEDGMENT

We thank the Australian Research Council for financial support.

■ REFERENCES

(1) Fujishima, A.; Honda, K. *Nature* **1972**, *238*, 37.

(2) Maruska, H. P.; Ghosh, A. K. *Sol. Energy* **1978**, *20*, 443.

(3) Heller, A. *Science* **1984**, *223*, 1141.

(4) Bard, A. J.; Fox, M. A. *Acc. Chem. Res.* **1995**, *28*, 141.

(5) Kudo, A. *Int. J. Hydrogen Energy* **2007**, *32*, 2673.

(6) Youngblood, W. J.; Lee, S. H. A.; Maeda, K.; Mallouk, T. E. *Acc. Chem. Res.* **2009**, *42*, 1966.

(7) Domen, K.; Hara, M.; Kondo, J. K.; Takata, T. *Bull. Chem. Soc. Jpn.* **2000**, *73*, 1307.

(8) Osterloh, H. E. *Chem. Mater.* **2008**, *20*, 35.

(9) Kudo, A.; Miseki, Y. *Chem. Soc. Rev.* **2009**, *38*, 253.

(10) Inoue, Y. *Energy Environ. Sci.* **2009**, *2*, 364.

(11) Maeda, K.; Teramura, K.; Lu, D.; Takata, T.; Saito, N.; Inoue, Y.; Domen, K. *Nature* **2006**, *440*, 295.

(12) Lee, Y.; Terashita, H.; Shimodaira, Y.; Teramura, K.; Hara, M.; Kobayashi, H.; Domen, K.; Yashima, M. *J. Phys. Chem. C* **2007**, *111*, 1042.

(13) Sayama, K.; Yoshida, R.; Kusama, H.; Okabe, K.; Abe, Y.; Arakawa, H. *Chem. Phys. Lett.* **1997**, *277*, 387.

(14) Abe, R.; Sayama, K.; Domen, K.; Arakawa, H. *Chem. Phys. Lett.* **2001**, *344*, 339.

(15) Sayama, K.; Mukasa, K.; Abe, R.; Abe, Y.; Arakawa, H. *J. Photochem. Photobiol., A* **2002**, *148*, 71.

(16) Kato, H.; Hori, M.; Konta, R.; Shimodaira, Y.; Kudo, A. *Chem. Lett.* **2004**, *33*, 1348.

(17) Abe, R.; Takata, T.; Sugihara, H.; Domen, K. *Chem. Commun.* **2005**, 3829.

(18) Kato, H.; Sasaki, Y.; Iwase, A.; Kudo, A. *Bull. Chem. Soc. Jpn.* **2007**, *12*, 2457.

(19) Higashi, M.; Abe, R.; Ishikawa, A.; Takata, T.; Ohtani, B.; Domen, K. *Chem. Lett.* **2008**, *37*, 138.

(20) Higashi, M.; Abe, R.; Teramura, K.; Takata, T.; Ohtani, B.; Domen, K. *Chem. Phys. Lett.* **2008**, *452*, 120.

(21) Sasaki, Y.; Nemoto, H.; Saito, K.; Kudo, A. *J. Phys. Chem. C* **2009**, *113*, 17536.

(22) Tabata, M.; Maeda, K.; Higashi, M.; Lu, D.; Takata, T.; Abe, R.; Domen, K. *Langmuir* **2010**, *26*, 9161.

(23) Ng, Y. H.; Lightcap, I. V.; Goodwin, K.; Matsumura, M.; Kamat, P. V. *J. Phys. Chem. Lett.* **2010**, *1*, 2222.

(24) Ng, Y. H.; Iwase, A.; Kudo, A.; Amal, R. *J. Phys. Chem. Lett.* **2010**, *1*, 2607.

(25) Lightcap, I. V.; Kosel, T. H.; Kamat, P. V. *Nano Lett.* **2010**, *10*, 577.

(26) Apparent quantum yield = 100% × [(no. of evolved H_2 molecules) × 4]/(no. of incident photons).

(27) Assuming that the PRGO contains partially oxidized carbon (greater molecular weight) would give a TON > 3.2 because the TON is determined by the number of moles of reactive electrons per mole of PRGO. Assuming that the PRGO contains pristine graphitic carbon ensures that our calculated TON of 3.2 is not overestimated.

(28) Konta, R.; Ishii, T.; Kato, H.; Kudo, A. *J. Phys. Chem. B* **2004**, *108*, 8992.